Macromolecules

pubs.acs.org/Macromolecules Article

Anionic Ring-Opening Polymerization of a Functional Epoxide Monomer with an Oxazoline Protecting Group for the Synthesis of Polyethers with Carboxylic Acid Pendants

Jihye Park, Yeji Yu, Joo Won Lee, and Byeong-Su Kim*

Cite This: Macromolecules 2022, 55, 5448–5458 Read Online

ACCESS | Metrics & More | Article Recommendations | Supporting Information

ABSTRACT: Polymers with carboxylic acid functionalities are widely used in adhesives, absorbents, dispersants, drug delivery systems, and hydrogels. Unlike common radical polymerization, it is difficult to synthesize polymers with carboxylic acid groups via anionic ring-opening polymerization because of the harsh reaction conditions. Although a carboxylic acid-functionalized polyether, poly(glycidoxy acetic acid), was previously prepared by using monomer-activated ring-opening polymerization, this approach often suffers from a low initiation efficiency and is limited to homopolymerization. Herein, we present a novel functional epoxide monomer bearing oxazoline as a protecting group, 4,4-dimethyl-2-oxazoline glycidyl ether, for a controlled synthesis of poly(4,4-dimethyl-2-oxazoline glycidyl ether) by overcoming the aforementioned limitations. The stepwise syntheses of the monomer and polymers were carefully analyzed via ^{1}H NMR, GPC, FT-IR spectroscopy, and MALDI-ToF analysis. Furthermore, copolymerization with another monomer and a macroinitiator yielded well-defined polymers. We anticipate that this study will provide a new platform for the synthesis of polyethers with carboxylic acid functional groups.

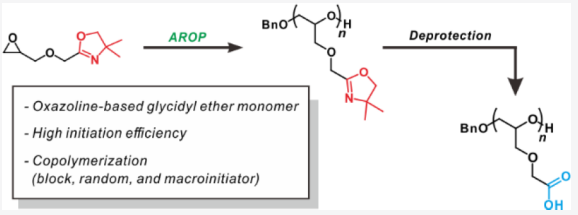

INTRODUCTION

Poly(ethylene glycol) (PEG) is the most representative class of aliphatic polyethers with a broad range of applications in the biological field and pharmaceutical industry because of its excellent solubility, biocompatibility, and low immunogenicity.[1−3] However, the limited functionality within the PEG backbone represents a fundamental challenge that prevents its widespread applications.[4] Significant progress has been made during the past decades in the development of efficient approaches to prepare functionalized polyethers containing diverse arrays of structures and functionalities.[5−9]

The most conventional synthetic approach for functional PEGs and their derivatives involves anionic ring-opening polymerization (AROP) of functional epoxide monomers. To date, a diverse array of epoxide monomers with unique functionalities have been developed, including azide,[9] allyl,[10] thiol,[11] and acetal functionalities.[12−15] However, many of these functional moieties are labile to direct polymerization under the harsh anionic polymerization conditions, resulting in undesirable side reactions and/or no polymerization.[16,17] Alternatively, monomer-activated ring-opening polymerization (MAROP) has been suggested to enable versatile approach to a diverse array of polyethers possessing sensitive functional groups by using an initiating complex of aluminum-based catalyst and a weakly nucleophilic quaternary ammonium-based initiator.[18−20] Nevertheless, novel functional epoxide monomers that can tolerate common AROP conditions are still highly desirable, in view of their wider utility for the creation of functional polyethers.

Polyanions, such as poly(carboxylic acid),[21−23] poly(sulfonic acid),[24,25] and polyphosphate,[26,27] represent one of the most unique classes of macromolecules. In particular, poly(carboxylic acid)s are useful in many fields because of their distinct intrinsic properties, such as hydrophilicity, pH responsibility, and hydrogen-bonding capability. For example, as one of the most widely used polysaccharides, alginic acid derived from brown seaweeds has a broad range of potential applications in food, medicines, environmental protection, and packaging.[21,28] In addition, because of its superior hydration and biocompatibility, hyaluronic acid found in the human skin is used in food, medical, pharmaceutical, and cosmetic industries.[22,29] As a synthetic analogue to these natural poly(carboxylic acid)s, poly(acrylic acid)s and poly(methacrylic acid)s are also widely employed in adhesives,[30] dispersants,[31] absorbents,[32] and drug delivery systems.[33,34]

Despite the significant progress made in the synthesis of poly(carboxylic acid)s, only a few studies reported the synthesis of polyethers possessing carboxylic acid function-

Received: April 13, 2022
Revised: June 9, 2022
Published: June 29, 2022

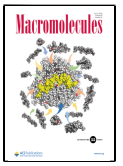

https://doi.org/10.1021/acs.macromol.2c00761
Macromolecules 2022, 55, 5448−5458

Scheme 1. Synthesis of Polyethers with Carboxylic Acid Pendant Groups

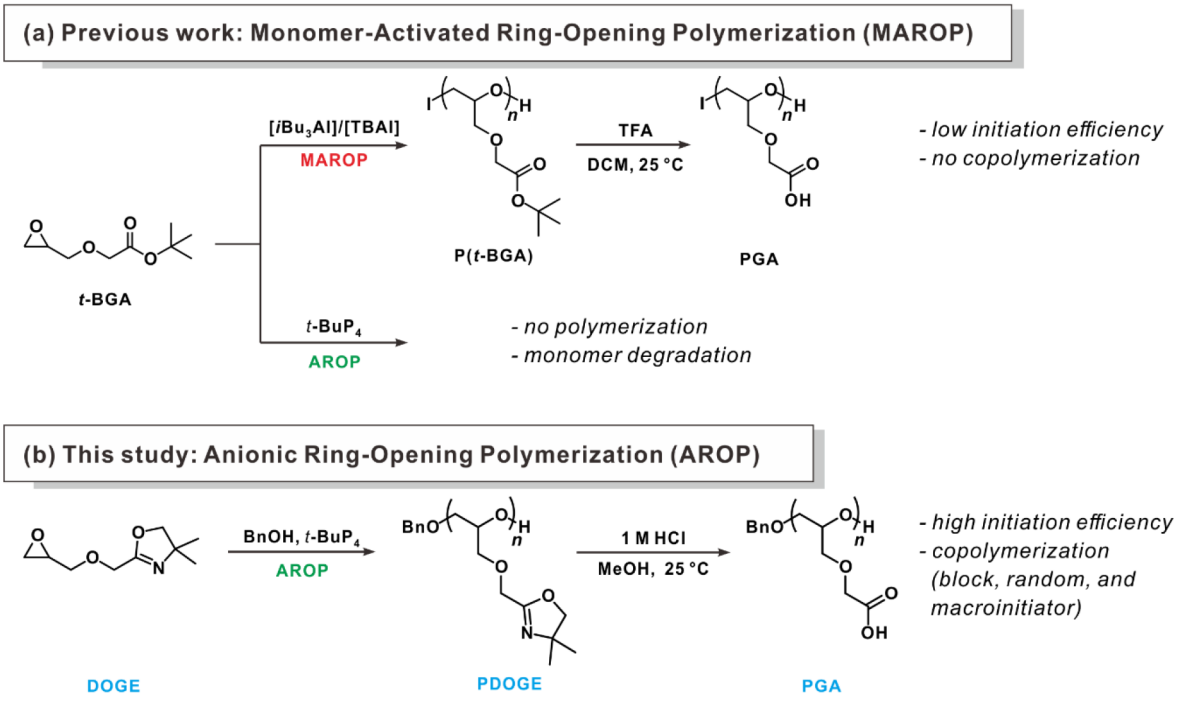

alities. Polyethers containing carboxylic acid groups have been recently introduced as a unique polymeric system combining both hydrogen-bonding acceptor and donor moieties within a single repeating unit; this enables the precise control of the cooperative hydrogen bonding, providing excellent adhesive property along with intrinsic biocompatibility.[20] However, because of the limited choice of functional monomers amenable to direct polymerization under the harsh conditions of anionic polymerization, postpolymerization modification via thiol−ene addition[35] and hydrolysis of nitrile groups[36] are typically employed in the synthesis of polyethers containing carboxylic acids. In this context, our group reported the direct synthesis of poly(glycidoxy acetic acid) (PGA) using MAROP of *tert*-butyl glycidoxy acetate monomers recently;[20] however, this approach suffered from a low initiation efficiency, resulting in limited fidelity in modification and conjugation with other chemical moieties and was only applied in homopolymerization (Scheme 1a). In another noteworthy effort, Frey and coworkers presented novel epoxide monomers, such as *tert*-butyl 4,5-epoxypentenoate and methyl 4,5-epoxypentenoate, for homo- and copolymerization with ethylene oxide via MAROP, affording polyethers with gradient and random distributions of carboxylic acid functionalities.[19]

To develop a facile and controllable synthetic method of polyethers bearing carboxylic acid pendant groups, herein we report a novel functional epoxide monomer containing the oxazoline ring as a protecting group for the carboxylic acid functionality, amenable to direct polymerization under the harsh conditions of anionic polymerization. Specifically, we introduced an oxazoline-bearing monomer, 4,4-dimethyl-2-oxazoline glycidyl ether (DOGE), to perform a controlled synthesis of poly(4,4-dimethyl-2-oxazoline glycidyl ether) (PDOGE) with a narrow molecular weight dispersity, followed by a subsequent acidic deprotection process to yield poly(glycidoxy acetic acid) (PGA), alleviating the aforementioned limitations (Scheme 1b). The stepwise syntheses of the monomer and polymers were carefully analyzed through ^{1}H NMR, gel permeation chromatography (GPC), and Fourier-transform infrared (FT-IR) spectroscopies as well as matrix-assisted laser desorption and ionization time-of-flight (MALDI-ToF) analysis. Furthermore, copolymerization with other common monomers, such as allyl glycidyl ether, and polymerization using a poly(ethylene oxide) (PEO) macroinitiator were demonstrated to yield well-defined random and block copolymers. We anticipate that this study will open new avenues for the synthesis of polyethers with carboxylic acid functionality.

EXPERIMENTAL SECTION

Materials. All the materials used in this study were purchased from commercial chemical suppliers (Sigma-Aldrich, TCI Chemicals, Thermo Fisher Scientific, Acros Organics, and SAMCHUN Chemicals), unless otherwise stated. Deuterated $CDCl_3$ and MeOD NMR solvents were purchased from Cambridge Isotope Laboratory.

Characterizations. ^{1}H, ^{13}C, correlation spectroscopy (COSY), and heteronuclear single-quantum correlation (HSQC) NMR spectra were recorded on a Bruker 400 MHz spectrometer at 25 °C. $CDCl_3$ (δH = 7.26 ppm and δC = 77.16 ppm) and MeOD (δH = 3.31 ppm and δC = 49.00 ppm) were used as internal standards. The number-average (M_n) and weight-average (M_w) molecular weights and corresponding molecular weight distribution (M_w/M_n, $Đ$) were measured through GPC by using an Agilent 1200 series with THF as eluent at 25 °C and a flow rate of 1.00 mL min^{-1}with a refractive index (RI) detector. All calibrations were performed by using polystyrene (PS) standards (Sigma-Aldrich; M_p, 250−1100000). FT-IR spectra were recorded on an Agilent Cary 630 spectrometer with an attenuated total reflection (ATR) module. MALDI-ToF mass spectrometry (MS) measurements were performed by using *trans*-2-[3-(4-*tert*-butylphenyl)-2-methyl-2-propenylidene]malononitrile as a matrix on a Bruker Autoflex Max instrument. Differential scanning calorimetry (DSC) (Q200 model, TA Instruments) was employed under a nitrogen atmosphere from −80 to 150 °C with a heating rate of 10 °C min^{-1}. Prior to the measurement, the sample was annealed, and the second cycle was used to determine the thermal properties of the resulting polymers.

https://doi.org/10.1021/acs.macromol.2c00761
Macromolecules 2022, 55, 5448−5458

Scheme 2. Representative Scheme for the Synthesis of (a) DOGE Monomer and (b) PDOGE Homopolymer with Subsequent Deprotection for the Synthesis of PGA

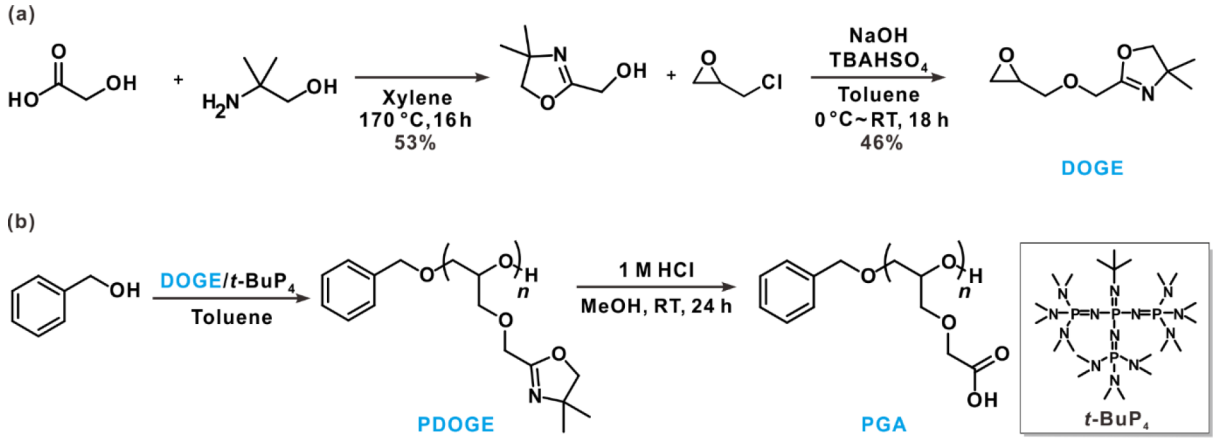

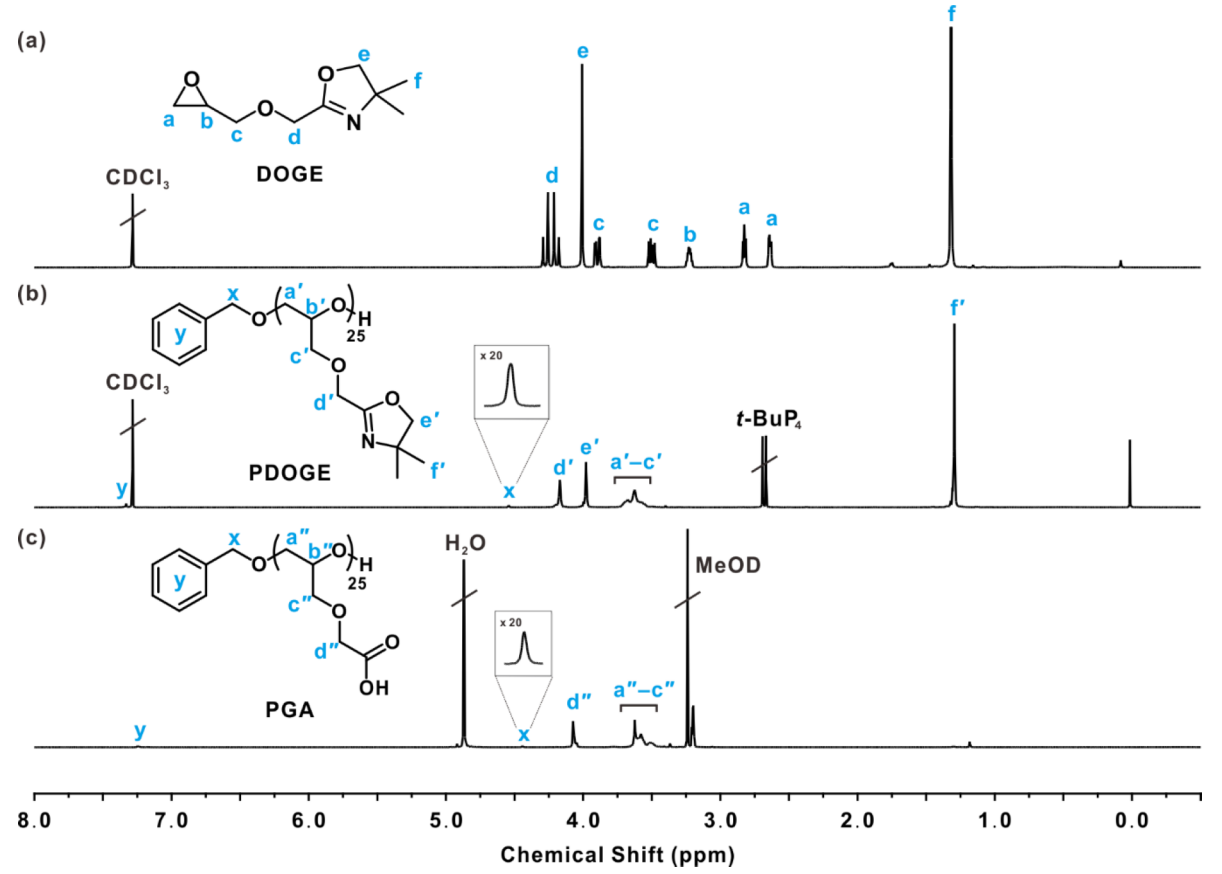

Figure 1. Representative ^{1}H NMR spectra of (a) DOGE monomer, (b) $PDOGE_{25}$ homopolymer (entry 1 in Table 1), and (c) deprotected PGA_{25}. See the Experimental Section for details.

Synthesis of (4,4-Dimethyl-4,5-dihydrooxazol-2-yl)-methanol. The synthesis of (4,4-dimethyl-4,5-dihydrooxazol-2-yl)methanol was performed according to a method reported in the literature with slight modifications.[37] Glycolic acid (5.97 g, 78.5 mmol) was added to a solution of 2-amine-2-methyl-1-propanol (7.49 mL, 78.5 mmol) in 125 mL of xylene in a 250 mL round-bottom flask equipped with a Dean−Stark apparatus and heated to 170 °C for 16 h. Xylene was removed under reduced pressure. Afterward, the obtained yellow viscous mixture was purified by sublimation to yield white solid crystals of (4,4-dimethyl-4,5-dihydrooxazol-2-yl)methanol (4.69 g, 36.30 mmol, 46.2% yield). ^{1}H NMR (400 MHz, $CDCl_3$): δ 1.29 (s, 6H), 4.02 (s, 2H), 4.22 (s, 2H).

Synthesis of 4,4-Dimethyl-2-oxazoline Glycidyl Ether (DOGE). In a 500 mL round-bottom flask, 13.07 g of NaOH was dissolved in 19.60 mL of water to prepare a 40% aqueous NaOH solution, which was cooled in an ice bath to 0 °C. Tetrabutylammonium hydrogen sulfate ($TBAHSO_4$; 0.62 g, 1.82 mmol) and (4,4-dimethyl-4,5-dihydrooxazol-2-yl)methanol (4.69 g, 36.30 mmol) were added to the NaOH solution and stirred for 30 min at 0 °C. After that, epichlorohydrin (14.23 mL, 181.50 mmol) was added slowly at 0 °C; the reaction mixture was stirred for 18 h and then heated to 25 °C. After extracting the reaction mixture with ethyl acetate, the organic layer was dried over Na_2SO_4 and concentrated *in vacuo*. The crude product was stored over CaH_2 for 12 h to remove moisture, followed by distillation to yield a yellow oil product (3.00 g, 16.20

https://doi.org/10.1021/acs.macromol.2c00761
Macromolecules 2022, 55, 5448−5458

Table 1. Characterizations of the Synthesized PDOGE

entry	temp (°C)	DOGE (equiv)	time (h)	conv[a] (%)	$M_{n,th}$ (g/mol)	$M_{n,NMR}$[b] (g/mol)	$M_{n,GPC}$[c] (g/mol)	$Đ$[c]	T_g[d] (°C)
1	0	25	12	>99	4740	4740	3600	1.07	n.d.
2		50	24	>99	9370	9370	6030	1.06	n.d.
3		100	36	72	13440	13260	5800	1.08	n.d.
4	25	25	4	>99	4740	4740	2900	1.09	−18.9
5		50	4	>99	9370	9370	4430	1.10	−16.2
6		100	8	>99	18630	21220	6100	1.08	−15.6
7		200	36	97	37150	39930	5200	1.15	−13.2

[a]DOGE conversion as determined by using ^{1}H NMR spectra of crude mixture. [b]Determined from ^{1}H NMR spectra of isolated polymer ($CDCl_3$, 400 MHz). [c]Determined from GPC in THF by using an RI signal and a PS standard. [d]Determined by the differential scanning calorimetry (DSC) at a rate of 10 °C/min.

mmol, 44.6% yield). ^{1}H NMR (400 MHz, $CDCl_3$): δ 4.22 (m, 2H), 3.99 (s, 2H), 3.87 (dd, J = 11.7, 3.1 Hz, 1H), 3.50 (dd, J = 11.7, 5.9 Hz, 1H), 3.21 (m, J = 5.9, 4.1, 2.9 Hz, 1H), 2.81 (dd, J = 4.9, 4.2 Hz, 1H), 2.62 (dd, J = 5.0, 2.7 Hz, 1H), 1.30 (s, 6H). ^{13}C NMR (101 MHz, $CDCl_3$): δ 162.03, 79.24, 72.05, 67.20, 65.68, 50.47, 44.18, 28.27. Electrospray ionization mass spectrometry (ESI-MS) (m/z): $[M + H]^+$ calcd for $C_9H_{15}NO_3$, 185.11; obsd 186.11.

Synthesis of Poly(4,4-Dimethyl-2-oxazoline glycidyl ether) (PDOGE). A mixture of t-BuP_4 (0.8 M in hexane, 1.2 equiv) and benzyl alcohol (1.0 equiv) in toluene (2.5 M relative to the monomer) was stirred for 30 min. The mixture was cooled in an ice bath to 0 °C, and then DOGE (500 mg, 2.7 mmol, 25 equiv) was slowly injected to the mixture for the initiation of the polymerization. The completion of the polymerization was determined via ^{1}H NMR by checking the residual epoxide peaks of the monomer. Polymerization was terminated by adding an excess amount of methanol. The polymer was concentrated *in vacuo* to obtain a yellow oil corresponding to PDOGE (entry 1 in Table 1). ^{1}H NMR (400 MHz, $CDCl_3$): δ 7.37−7.33 (m, 5H), 4.53 (s, 2H), 4.16 (s, 50H), 3.96 (s, 50H), 3.70−3.58 (m, 125H), 1.29 (s, 150H).

Deprotection of PDOGE. PDOGE (450 mg, 1.0 equiv of oxazoline moiety) was reacted with 1.0 M HCl (5.0 equiv with respect to the oxazoline moiety) in methanol (1:1, v/v %). The mixture was reacted at 25 °C for 24 h. Complete deprotection was confirmed by ^{1}H NMR. Residual HCl was removed *in vacuo*, and the mixture was treated with Amberlite IR-120(H) to remove t-BuP_4. The residual oily product was dissolved in methanol and purified by precipitation in cold 1.0 M HCl, to prepare a white oil of the deprotected PGA polymer derived from PDOGE (entry 1 in Table 1). ^{1}H NMR (400 MHz, MeOD): δ 7.41−7.22 (m, 5H), 4.55 (s, 2H), 4.26−4.09 (m, 50H), 3.89−3.50 (m, 125H). ^{13}C NMR (101 MHz, MeOD): δ 172.70, 80.05, 72.55, 70.78, 69.43.

Synthesis of Copolymers. *Synthesis of P(DOGE-b-AGE).* A mixture of t-BuP_4 (0.8 M in hexane, 162 μL, 0.130 mmol, 1.2 equiv) and benzyl alcohol (11.23 μL, 0.108 mmol, 1.0 equiv) in toluene (0.42 mL, 2.5 M relative to the DOGE monomer) was stirred for 30 min. Then, DOGE (500 mg, 2.70 mmol, 25 equiv) was added dropwise to the mixture, while monitoring the polymerization via ^{1}H NMR. We determined the completion of the reaction using ^{1}H NMR by checking the residual epoxide signals of the monomer. After it was confirmed that the DOGE monomer was completely consumed, allyl glycidyl ether (AGE; 308 mg, 2.70 mmol, 25 equiv) was slowly added to the solution. The polymerization was terminated by adding an excess amount of methanol after the reaction was completed. The polymer was then concentrated *in vacuo* to yield the desired polymer. ^{1}H NMR (400 MHz, $CDCl_3$): δ 7.32 (s, 5H), 5.88 (ddd, J = 22.4, 10.6, 5.5 Hz, 25H), 5.26 (dd, J = 17.2, 1.6 Hz, 25H) 5.16 (dd, J = 10.4, 1.6 Hz, 25H), 4.53 (s, 2H), 4.15 (s, 50H), 3.97 (two s, 100H), 3.57 (m, 250H), 1.27 (s, 150H) (entry 2 in Table 2).

Synthesis of P(DOGE-co-AGE). A mixture of benzyl alcohol (11.23 μL, 0.108 mmol, 1.0 equiv), DOGE (500 mg, 2.70 mmol, 25 equiv), and AGE (308 mg, 2.70 mmol, 25 equiv) in toluene (1.18 mL, 2.5 M relative to the monomers) was stirred. Then, t-BuP_4 (0.8 M in hexane, 162 μL, 0.130 mmol, 1.2 equiv) was added to the mixture, and the reaction was monitored by ^{1}H NMR. The completion of the reaction was determined by using ^{1}H NMR to check the residual epoxide peaks of the monomer. The polymerization was terminated by adding an excess amount of methanol after the reaction was completed. Then, the polymer was concentrated *in vacuo* to yield the desired polymer. ^{1}H NMR (400 MHz, $CDCl_3$): δ 7.32 (s, 5H), 5.88 (ddd, J = 22.4, 10.6, 5.5 Hz, 25H), 5.26 (dd, J = 17.2, 1.6 Hz, 25H) 5.16 (dd, J = 10.4, 1.6 Hz, 25H), 4.53 (s, 2H), 4.15 (s, 50H), 3.97 (two s, 100H), 3.57 (m, 250H), 1.27 (s, 150H) (entry 3 in Table 2).

Deprotections of Copolymers. Copolymer (470 mg, 1.0 equiv of oxazoline moiety) was reacted with 1.0 M HCl (5.0 equiv with respect to the oxazoline moiety) in methanol (1:1, v/v %). The mixture was reacted at 25 °C for 24 h. Complete deprotection was confirmed by ^{1}H NMR. Residual HCl was removed *in vacuo*, and the mixture was treated with Amberlite IR-120(H) to remove t-BuP_4. The residual oil was dissolved in methanol and precipitated into a cold ethyl ether to prepare a white oil of the deprotected copolymers. ^{1}H NMR (400 MHz, MeOD): δ 7.25 (d, J = 4.7 Hz, 5H), 5.88−5.74 (m, 25H), 5.12 (dd, J = 49.1, 13.7 Hz, 50H), 4.44 (s, 2H), 4.10 (d, J = 12.0 Hz, 50H), 3.91 (d, J = 5.1 Hz, 50H), 3.74−3.34 (m, 250H).

***In Situ* ^{1}H NMR Polymerization Kinetics.** A mixture of benzyl alcohol initiator (1.0 equiv), DOGE monomer (25 equiv), and AGE monomer (25 equiv) in toluene-d_8 (2.5 M relative to the monomers) was transferred to a NMR tube sealed with a rubber septum. Afterward, 1.2 equiv of t-BuP_4 was introduced to the NMR tube and mixed thoroughly, before being analyzed via NMR spectroscopy. The analysis temperature was set to 27 °C, and spectra were collected every 15 min with a total of 16 scans over 6 h. The integrals of the allylic proton of the AGE monomer (δ = 5.74 ppm) and methylene protons of DOGE (δ = 3.98 ppm) were checked to calculate the monomer conversion with regard to the residual peak of toluene (δ = 2.09 ppm) as internal standard.

Synthesis of PDOGE-*b*-PEO-*b*-PDOGE. A mixture of t-BuP_4 (0.8 M in hexane, 162 μL, 0.130 mmol, 2.4 equiv) and poly(ethylene oxide) (PEO; M_n: 10000 g mol^{-1}, 540.0 mg, 0.054 mmol, 1.0 equiv) in toluene (1.00 mL) was stirred for 30 min in 60 °C. The mixture was cooled to 40 °C, and then DOGE (500 mg, 2.70 mmol, 50 equiv) was dropwise added to the solution while the polymerization was monitored via ^{1}H NMR. The completion of the reaction was determined by using ^{1}H NMR to check the residual epoxide peaks of the monomer. After the polymerization was completed, the reaction was terminated by adding an excess amount of methanol, and the polymer was concentrated *in vacuo*. ^{1}H NMR (400 MHz, $CDCl_3$): δ 4.16 (s, 100H), 3.97 (s, J = 7.3 Hz, 100H), 3.73−3.50 (m, 346H), 1.28 (s, 300H) (entry 4 in Table 2).

Deprotection of PDOGE-*b*-PEO-*b*-PDOGE. PDOGE-*b*-PEO-*b*-PDOGE (entry 4 in Table 2) (1.10 g, 1.0 equiv of oxazoline moiety) was reacted with 1.0 M HCl (5.0 equiv with respect to the oxazoline moiety) in methanol (1:1, v/v %). The mixture was reacted at 25 °C for 24 h. Complete deprotection was confirmed by ^{1}H NMR. Residual HCl was removed *in vacuo*, and the mixture was treated with Amberlite IR-120(H) to remove t-BuP_4. The residual oil was dissolved in DCM and precipitated in a cold hexane through precipitation to prepare a white oil of the deprotected PGA-*b*-PEO-*b*-PGA. ^{1}H NMR (400 MHz, MeOD): δ 4.20 (s, 100H), 3.71 (d, J = 39.7 Hz, 1408H).

https://doi.org/10.1021/acs.macromol.2c00761
Macromolecules 2022, 55, 5448−5458

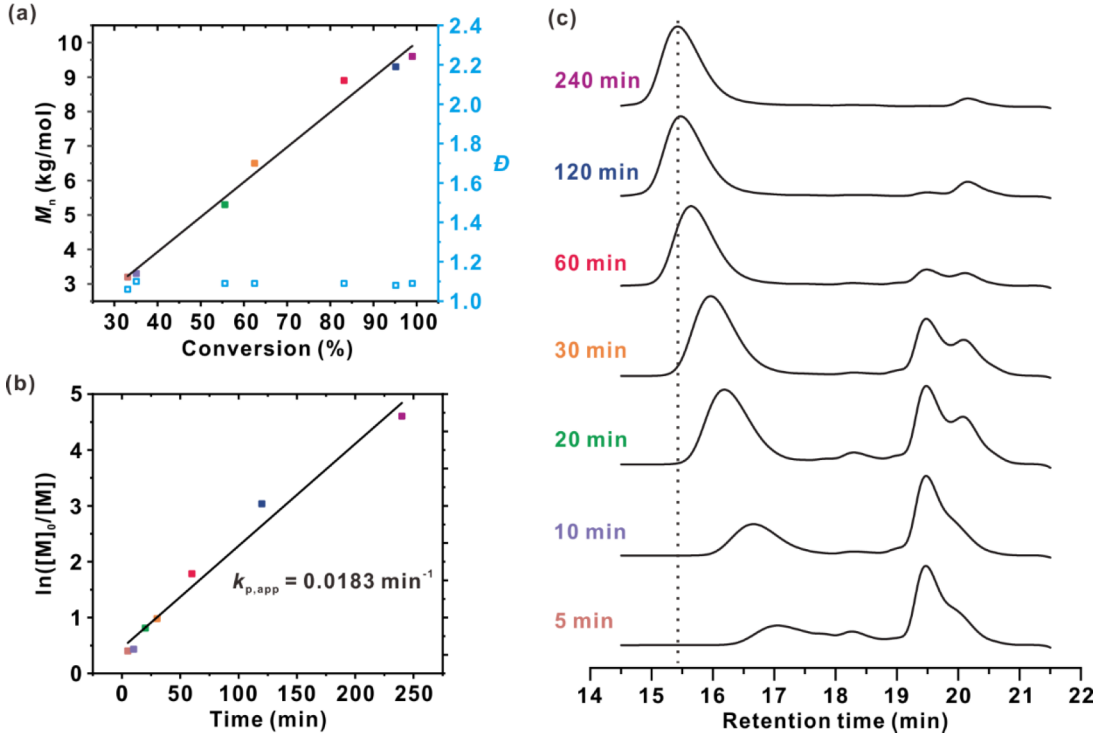

Figure 2. Polymerization kinetics of $PDOGE_{50}$ collected in toluene (2.5 M relative to DOGE) at 25 °C (entry 5 in Table 1). (a) Plot of $M_{n,NMR}$ and dispersity as a function of the total monomer conversion and (b) first-order kinetic plot of $\ln([M]_0/[M]_t)$ over polymerization time. (c) Evolution of corresponding GPC elugrams of samples collected at different polymerization times.

RESULTS AND DISCUSSION

Design and Synthesis of DOGE Monomer. To synthesize a polyether containing carboxylic acid functional groups, we designed an epoxide monomer with oxazoline as protecting group. The DOGE monomer, containing a protecting group for the carboxylic acid moiety, was synthesized through a simple two-step reaction (Scheme 2a). The initial reaction of 2-amine-2-methyl-1-propanol with glycolic acid, performed by using a Dean−Stark apparatus to capture H_2O as a byproduct, yielded the 4,4-dimethyl-2-oxazoline alcohol intermediate (Figure S1 in the Supporting Information). Interestingly, we found that controlling the reaction temperature and time was critical to increase the yield of the desired product due to the occurrence of 5,5-dimethyl-3-morpholinone as a side product (see Figure S1). Subsequently, a substitution reaction of the intermediate alcohol with epichlorohydrin produced the DOGE monomer, which was further purified by fractional distillation to an isolated yield of 45% (Scheme 2a). The chemical structure of the DOGE monomer was successfully verified through different NMR spectroscopic techniques, including ^{1}H NMR, ^{13}C NMR, correlation spectroscopy (COSY), heteronuclear single quantum correlation (HSQC), and electrospray ionization mass spectrometry (ESI-MS) (Figures 1a and S2−S5).

In contrast, our initial attempts using simple oxazoline derivatives without a dimethyl group, such as oxazoline and 4-methyl-2-oxazoline glycidyl ethers, were unsuccessful due to stability issues during the purification steps, which resulted in considerably low yields (Figures S6 and S7). Thus, we introduced two methyl groups in the oxazoline moiety to prevent the potential side reaction, in which the oxazoline ring is involved in the cationic ring-opening polymerization.[38]

Synthesis and Characterization of PDOGE. After its successful characterization, the DOGE monomer was subjected to polymerization via AROP to produce PDOGE in the presence of benzyl alcohol as initiator and *t*-BuP_4 as organic superbase catalyst. The highly basic organic base *t*-BuP_4 was selected for the reaction because it facilitated the controlled polymerization of the DOGE monomer under mild conditions (Scheme 2b). Considering the stability of DOGE, the initial polymerization was performed at 0 °C (entries 1−3 in Table 1). The DOGE monomer consumption was checked by using ^{1}H NMR to follow the disappearance of the methine and methylene protons of the epoxides (*a* and *b*) at 3.21, 2.81, and 2.62 ppm (Figure 1a). All proton peaks of PDOGE were assigned in the ^{1}H NMR spectrum, which displayed the characteristic peaks corresponding to the protons of the benzyl alcohol initiator (*x*) at 4.53 ppm and of the polymeric backbone at 3.70−3.58 ppm (Figure 1b). The degree of polymerization (DP) and the corresponding number-average molecular weight ($M_{n,NMR}$) of PDOGE were determined from the ratio of these two peaks. As shown in Table 1, the GPC analysis of the PDOGE homopolymers displayed a monomodal distribution with a narrow dispersity ($Đ$ = 1.06−1.08) for all the entries, indicating a controllable polymerization. It is of note that the $M_{n,GPC}$ values tended to be relatively lower than the $M_{n,NMR}$ ones, possibly due to the high hydrophobicity of the DOGE monomer; this difference became more pronounced as the DP of PDOGE increased, as similarly observed in previous studies.[15,39,40] In addition, the oxazoline moiety could interact with GPC column because of the basicity of oxazoline, which contributed to the underestimation of $M_{n,GPC}$. Furthermore, residual *t*-BuP_4 was still present even after a rigorous treatment using Amberlite IR-120(H) as an ion-exchange resin because of the potential interaction

https://doi.org/10.1021/acs.macromol.2c00761
Macromolecules 2022, 55, 5448−5458

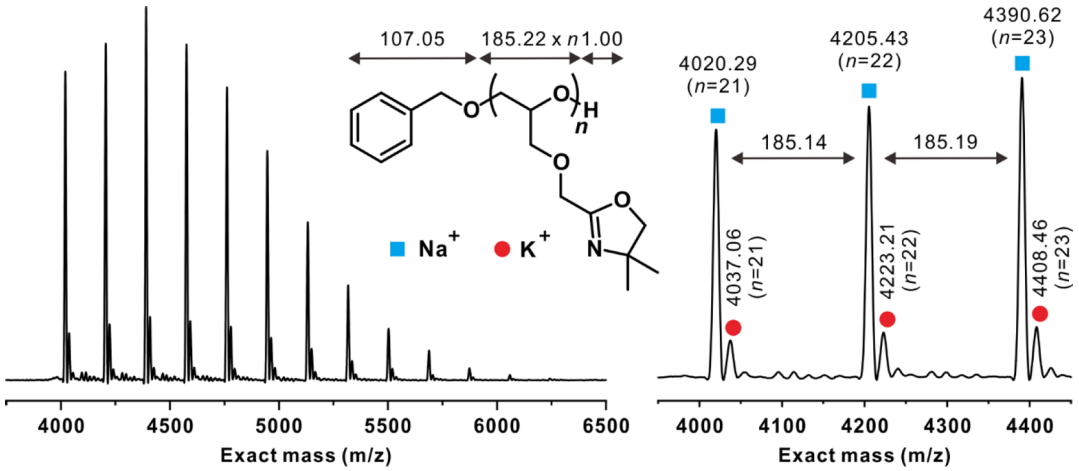

Figure 3. Representative MALDI-ToF mass spectrum of $PDOGE_{25}$ homopolymer (entry 1 in Table 1) synthesized with individual peak assignments in the selected region. Experimental conditions: positive mode, *trans*-2-[3-(4-*tert*-butylphenyl)-2-methyl-2-propenylidene]-malononitrile matrix; Na^+ (squares) and K^+ (circles) cationizing ions.

between the protonated *t*-BuP_4 and the nitrogen atoms of the oxazoline moiety in PDOGE. Complete removal of the residual *t*-BuP_4 was successfully observed after the deprotection of the oxazoline moiety, as shown in the ^1H NMR spectrum (Figure 1c).

Deprotection of PDOGE was conducted by hydrolysis under 1.0 M HCl condition, yielding PGA (Scheme 2b). As shown in Figure 1, the ^1H NMR spectrum shows that the characteristic oxazoline protons at 3.96 ppm disappeared after the deprotection. In addition, the deprotection was verified by ^{13}C NMR spectroscopy (Figure S8). Further details on the deprotected PGA are described in the following section.

Despite the stability issues of the monomer, DOGE could be polymerized in a controlled manner at 25 °C, as confirmed by ^1H NMR and GPC analyses (entries 4–7 in Table 1). The AROP of DOGE proceeded smoothly, achieving >99% conversion within 8 h, producing PDOGE with a controlled molecular weight and narrow dispersity ($Đ$ < 1.10). Although the polymerization to $PDOGE_{200}$ was not completed even after a prolonged polymerization time at 25 °C, the reaction generally produced PDOGE polymers with a well-defined molecular weight and narrow dispersity at a fast reaction rate.

To further evaluate the controlled polymerization of PDOGE, the polymerization kinetics running in toluene at 25 °C was examined via ^1H NMR and GPC (Figure 2). The monomer conversion, calculated from the evolution of the methylene proton signal of DOGE at 2.81 ppm, reached >99% within 4 h (entry 5 in Table 1). The linear correlation between $M_{n,NMR}$ and total monomer conversion, together with the low $Đ$ values, supported the controllable polymerization of PDOGE (Figure 2a). Moreover, the linear correlation between $\ln([M]_0/[M]_t)$ and the polymerization time indicated the complete living characteristics of the AROP of DOGE, exhibiting an apparent propagation rate constant ($k_{p,app}$) of 18.3×10^{-3} min^{-1} (Figure 2b). This value is ~3 times higher than that observed for the AROP of azidobutyl glycidyl ether (6.47×10^{-3} min^{-1}) in a previous study.[9] In parallel, the propagation rate constants (k_p) of glycidyl ether derivatives, determined from the $k_{p,app}/[I]_0$ ratio of the respective monomer by using the *t*-BuP_4 base, were 3.00×10^{-1} L mol^{-1} min^{-1} for allyl glycidyl ether, 2.23×10^{-1} L mol^{-1} min^{-1} for ethoxyethyl glycidyl ether, and 4.12×10^{-1} L mol^{-1} min^{-1} for benzyl glycidyl ether.[41] These values are similar to the k_p of 3.66×10^{-1} L mol^{-1} min^{-1} determined for the present DOGE system, indicating a reaction rate comparable to that of other epoxide monomers. As shown in Figure 2c, the molar mass distribution of PDOGE shifted toward a lower retention time as the polymerization proceeded, indicating that the polymer chain length increased during propagation and nearly saturated after 4 h.

Moreover, MALDI-ToF spectrometry was employed to evaluate the controlled polymerization of PDOGE and for end-group analysis (Figure 3). The MALDI-ToF spectrum of PDOGE displayed a single mass distribution with a constant interval of 185.22 g mol^{-1} corresponding to the molar mass of DOGE, demonstrating the successful incorporation of the functional monomer. The representative mass spectrum with the obtained molecular weight of 4205.43 g mol^{-1} corresponded to the PDOGE homopolymer, comprising the benzyl alcohol initiator (108.06 g mol^{-1}) and 22 monomers (185.22 g mol^{-1}), with Na^+ as the counterions. Irrespective of the type of counterions present, all peaks in the spectrum originated from the benzyl alcohol initiator, indicating a highly controllable initiation with a markedly higher efficiency than that reported in previous studies using MAROP.[20,42] A high initiation efficiency is critical when considering the reliability of initiators with other functionalities and of the conjugation of the prepared PDOGE polymers with other chemical moieties.

Deprotection of PDOGE. The prepared PDOGE and the deprotected PGA polymer were analyzed by FT-IR spectroscopy. The characteristic peak at 904 cm^{-1} corresponding to the epoxide moiety of DOGE disappeared, while the imine peak of the oxazoline moiety at 1667 cm^{-1} was retained after polymerization to PDOGE, indicating its successful synthesis without the degradation of the oxazoline moiety. Furthermore, the imine peak disappeared upon deprotection to PGA; this was accompanied by the observation of the carbonyl and hydroxy peaks at 1740 and 3563 cm^{-1}, respectively, and of the phenyl peak from the initiator at 1630 cm^{-1}; these results confirmed the preparation of the desired PGA product with the liberation of the carboxylic acid group (Figure 4).

The GPC analysis of PGA was limited due to potential interaction of carboxylic acid moieties with the GPC column. However, to determine $M_{n,GPC}$ of the deprotected PGA

https://doi.org/10.1021/acs.macromol.2c00761
Macromolecules 2022, 55, 5448–5458

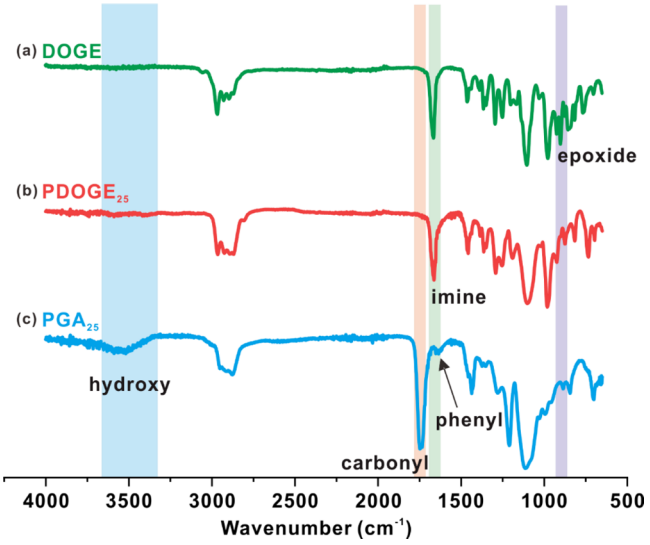

Figure 4. FT-IR spectra of (a) DOGE monomer, (b) $PDOGE_{25}$ homopolymer (entry 1 in Table 1), and (c) PGA_{25} with the assignments of characteristic peaks.

polymer indirectly, esterified PGA_{50} was synthesized by using trimethylsilyldiazomethane in methanol as confirmed by the ^{13}C NMR spectrum (Figure S9).[43] While the $M_{n,GPC}$ value of the methyl ester of PGA_{50} still showed a moderate difference with the $M_{n,NMR}$, the $Đ$ value does not vary considerably from that of $PDOGE_{50}$, indicating successful deprotection and controlled conversion (Figure S10).

Differential scanning calorimetry (DSC) analysis was used to evaluate the thermal property of the PDOGE polymers. The glass transition temperature (T_g) of the obtained polymers increased from −18.9 to −13.2 °C as the DP of PDOGE increased from 25 to 200 (Table 1 and Figure S11). These T_g values are in a similar range to those of other polyethers with pendant functional groups, such as *tert*-butyl acetate.[20] In addition, the T_g value of $PDOGE_{25}$ showed a significant increase from −18.9 to −7.85 °C upon deprotection to PGA_{25}, suggesting the presence of hydrogen-bonding interactions between the polymer chains at both inter- and intramolecular levels, as demonstrated in a previous study (Figure S11).[20]

Copolymerization of DOGE. To demonstrate the versatility of the DOGE monomer, we performed its copolymerization with AGE, one of the most widely used commercial epoxide monomers (Figure 5 and Table 2). First, a block copolymer, P(DOGE-*b*-AGE), was prepared by sequential addition of AGE monomer after the DOGE polymerization at 25 °C (entry 2 in Table 2). The ^1H NMR spectrum of P(DOGE-*b*-AGE) clearly exhibited the characteristic peaks originating from each monomer (Figure S12). Furthermore, the GPC trace shifted to higher molecular weights after the addition of the AGE monomer, indicating the successful block copolymerization of the desired P(DOGE-*b*-AGE) polymer; no unreacted chain ends of PDOGE were present, as evidenced by the absence of the shoulder peak (Figure 5a). Along with the low $Đ$ value of the block copolymer, this observation clearly demonstrates the living characteristics of the propagating chain end of PDOGE. In parallel, the copolymerization in a reverse sequence of monomer addition provided a well-defined diblock copolymer of $P(AGE_{25}$-*b*-$DOGE_{25})$ (Figure S13). It should be noted that the successful preparation of a well-defined block copolymer achieved in this study is challenging for MAROP systems because of their poor initiation efficiency.[20]

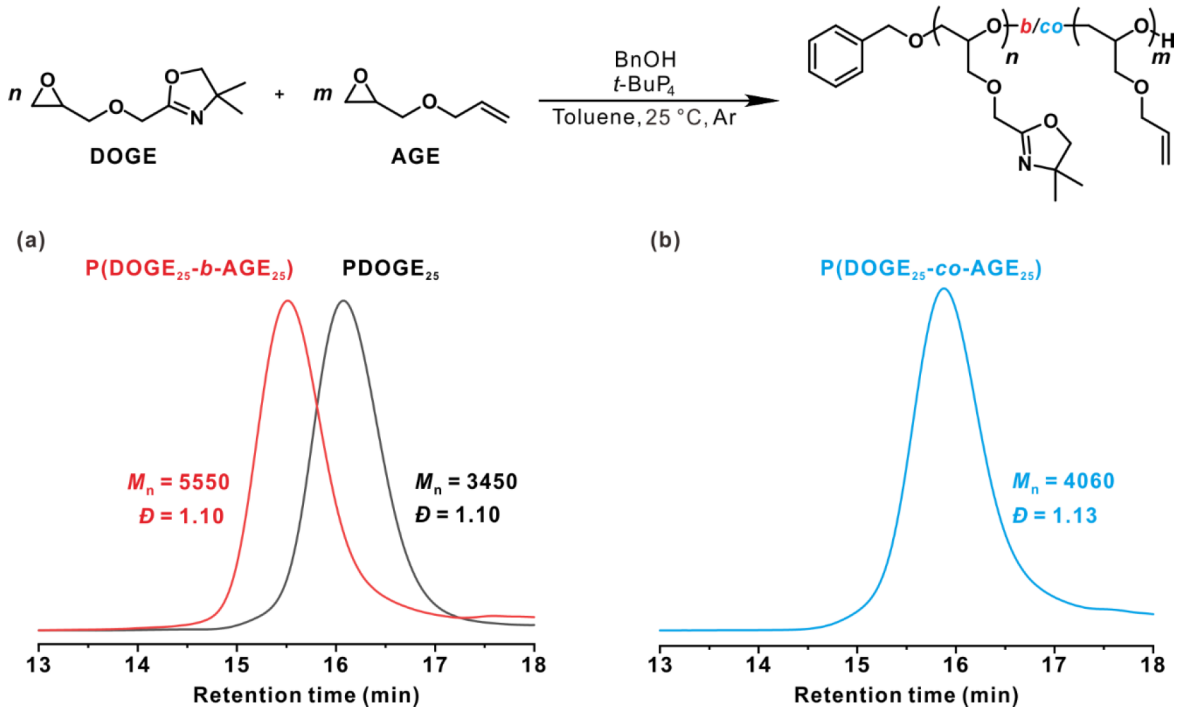

Figure 5. Copolymerization of DOGE with AGE to synthesize $P(DOGE_{25}$-*b*-$AGE_{25})$ (entry 2 in Table 2) and $P(DOGE_{25}$-*co*-$AGE_{25})$ (entry 3 in Table 2). (a) GPC traces of $PDOGE_{25}$ (black), $P(DOGE_{25}$-*b*-$AGE_{25})$ (red), and (b) $P(DOGE_{25}$-*co*-$AGE_{25})$ (blue), with the corresponding $M_{n,GPC}$ and $Đ$ values measured in THF.

https://doi.org/10.1021/acs.macromol.2c00761
Macromolecules 2022, 55, 5448−5458

Table 2. Characterization Data for All the Copolymers Prepared in This Study

entry	polymer composition	temp (°C)	time (h)	conv[b] (%)	$M_{n,th}$ (g/mol)	$M_{n,NMR}$[c] (g/mol)	$M_{n,GPC}$[d] (g/mol)	$Đ$[d]	T_g[e] (°C)
1	$PDOGE_{25}$[a]	25	4	>99	4740	4740	3450	1.10	−18.9
2	$P(DOGE_{25}$-*b*-$AGE_{25})$	25	8	>99	7600	7710	5550	1.10	−48.1
3	$P(DOGE_{25}$-*co*-$AGE_{25})$	25	8	>99	7600	7180	4060	1.13	−44.2
4[f]	$PDOGE_{25}$-*b*-PEO-*b*-$PDOGE_{25}$	40	12	>99	19260	19260	16940	1.10	−18.5, 52.5[g]

[a]First block polymer of $P(DOGE_{25}$-*b*-$AGE_{25})$. [b]AGE and DOGE conversion, as determined from ^{1}H NMR spectra of a crude mixture. [c]Determined from ^{1}H NMR spectra of isolated polymer ($CDCl_3$, 400 MHz). [d]Determined by GPC in THF using RI signal and PS standard. [e]Measured via DSC. [f]Prepared using PEO with M_n = 10000 g mol^{-1}. [g]T_m of resulting $PDOGE_{25}$-*b*-PEO-*b*-$PDOGE_{25}$.

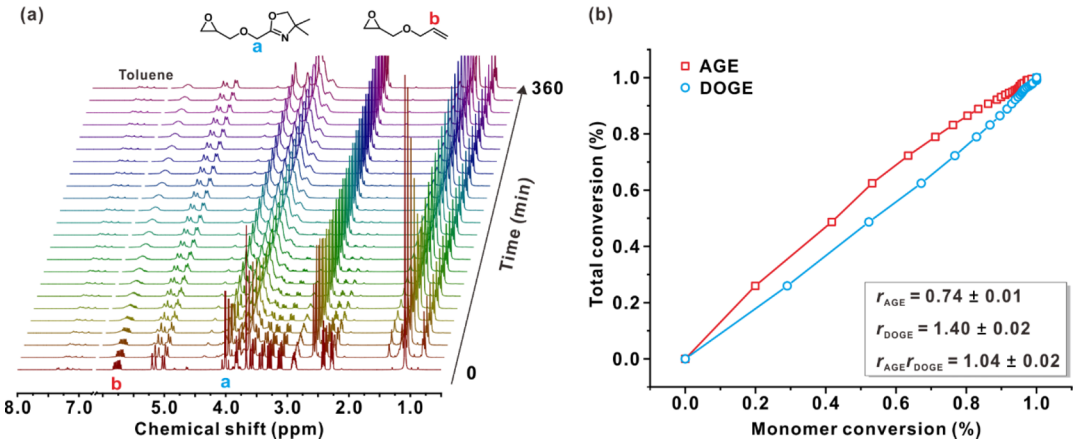

Figure 6. (a) Time-resolved ^{1}H NMR spectra obtained during the copolymerization of DOGE and AGE in 2.5 M toluene-d_8 at 27 °C. (b) Total polymerization conversion with respect to monomer conversion for copolymerization of DOGE (blue open circles) and AGE (red open squares). Initial fractions: n_{DOGE} = 0.57 and n_{AGE} = 0.43.

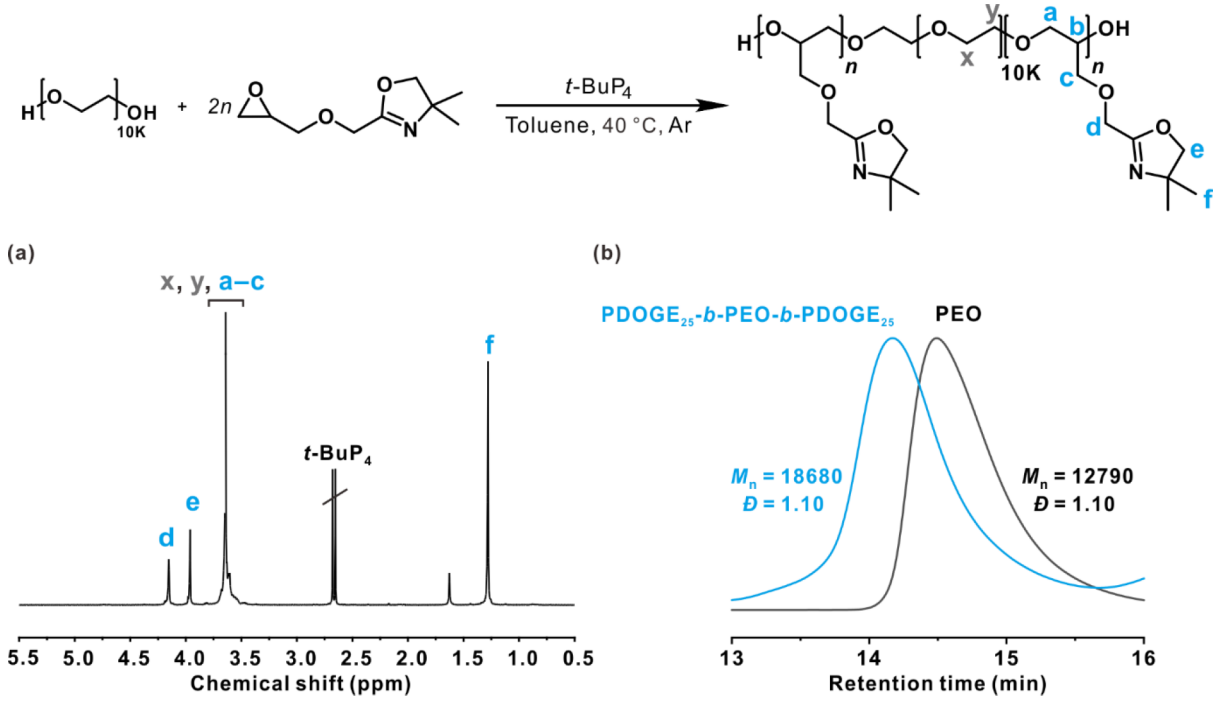

Figure 7. Polymerization of the DOGE monomer using the PEO macroinitiator (entry 4 in Table 2). (a) ^{1}H NMR spectrum and (b) GPC profile of PEO (black) and $PDOGE_{25}$-*b*-PEO-*b*-$PDOGE_{25}$ (blue) with the corresponding $M_{n,GPC}$ and $Đ$ values measured in THF.

Moreover, a desired statistical copolymer, P(DOGE-*co*-AGE), was synthesized by use of the living characteristics of the polymerization using the two monomers in a one-pot reaction (entry 3 in Table 2). The ^{1}H NMR spectrum of the prepared copolymer displayed the characteristic peaks of both oxazoline moiety and allyl groups (Figure S14). Moreover, the GPC analysis of P(DOGE-*co*-AGE) showed a monomodal distribution with narrow dispersity ($Đ$ = 1.13) (Figure 5b). This is in clear contrast with a previous copolymerization study

https://doi.org/10.1021/acs.macromol.2c00761
Macromolecules 2022, 55, 5448−5458

using MAROP, which reported a bimodal distribution originating from undesired initiation.[19]

The DSC analysis showed that both block and random copolymers had similar T_g values of −48.1 and −44.2 °C, respectively (Table 2 and Figure S15). Interestingly, considering the weight fractions of the respective blocks within the copolymer and the T_g values of the corresponding homopolymers (i.e., $PDOGE_{25}$: −18.9 °C; PAGE: −77 °C),[35] a T_g of −44.7 °C was calculated on the basis of the Fox equation,[44] in concert with the observed T_g value of the copolymer.

To elucidate the microstructure of the P(DOGE-*co*-AGE) copolymer, the reactivity ratios of DOGE and AGE during the copolymerization were further examined by *in situ* ^{1}H NMR spectroscopy (Figure 6). Statistical copolymerization of DOGE and AGE in toluene-d_8 was conducted in an NMR tube. Both monomer conversions and total conversions were measured as a function of time, from which the reactivity ratios of DOGE and AGE were determined by using the nonterminal model of chain copolymerization developed by Lynd and co-workers.[45] In particular, the methylene peak of DOGE (*a*, 3.98 ppm) and the allylic peak of AGE (*b*, 5.74 ppm) were integrated to obtain the monomer conversion relative to the toluene peak at 2.09 ppm as an internal standard (Figure 6a). The plot of total vs monomer conversion was used to extract the following reactivity ratios for the pair of monomers: $r_{DOGE} = 1.40 \pm 0.02$ and $r_{AGE} = 0.74 \pm 0.01$, which denoted an almost ideal statistical copolymerization ($r_{AGE} \times r_{DOGE} = 1.04 \pm 0.02$) (Figure 6b).

Subsequently, deprotection of each copolymer was performed by further treatment with 1.0 M HCl. In all cases, the characteristic peaks of the PGA polymer were observed via ^{1}H NMR and FT-IR analyses, which indicated that deprotection was successfully achieved, while leaving the allyl group intact (Figures S16−S19). This feature promises potential for an orthogonal functionalization to provide a diverse array of functional polymers on the PGA copolymer platform.

Encouraged by the well-defined copolymerization of the DOGE monomer discussed above, we extended the present approach to highlight the controllable initiation process using *α*,*ω*-dihydroxy-terminated PEO (M_n = 10 kDa) as macroinitiator at 40 °C (Figure 7 and entry 4 in Table 2). The chemical structure of the resulting ABA-type triblock copolymer, PDOGE-*b*-PEO-*b*-PDOGE, was successfully identified via ^{1}H NMR spectroscopy (Figure 7a). For example, the molecular weight and DP of the ABA triblock copolymer were determined by integrating the oxazoline protons at the 5-position of the DOGE monomer (peak *e*, 3.98 ppm) and polyether backbone (3.75−3.43 ppm). Moreover, the GPC profiles of the triblock copolymers showed a monomodal distribution with narrow dispersity ($Đ$ = 1.10), exhibiting a clear shift to the higher-molecular-weight region without any noticeable shoulder trace (Figure 7b). DSC analysis further provided the thermal properties of the resulting triblock copolymer (Figure S20). Interestingly, we observed a single T_g of −18.5 °C together with a T_m of 52.5 °C, suggesting the good miscibility of all polyether-based triblock copolymers, while retaining the highly crystalline nature of the PEO midblock within the ABA triblock copolymers.

Finally, the deprotection of PDOGE block within the triblock copolymer was conducted in the presence of 1.0 M HCl to produce the ABA triblock copolymer PGA-*b*-PEO-*b*-PGA containing carboxylic acid functionalities. The ^{1}H NMR spectrum showed the disappearance of the oxazoline protons at 3.75 ppm upon deprotection (Figure S21). Moreover, it was found that the characteristic oxazoline peak at 1666 cm^{-1} disappeared following the deprotection, with the concomitant appearance of the carbonyl peak at 1740 cm^{-1} (Figure S22). Taken together, these results show the successful preparation of the desired PGA-*b*-PEO-*b*-PGA triblock copolymer, which will find its utility in hydrogel and drug-delivery systems.

CONCLUSION

In summary, we developed a novel functional epoxide monomer, DOGE, for the synthesis of polyethers possessing carboxylic acid functionalities. Controlled AROP of the DOGE monomer proceeded without degradation of the oxazoline moiety, and the following acidic deprotection produced well-defined PGA in a highly controllable manner and without any side reactions. On the basis of its high initiation efficiency (as demonstrated via MALDI-ToF analysis), we successfully combined DOGE with the commercial AGE monomer to prepare well-defined block and statistical copolymers with a narrow dispersity, which could not be obtained in previous synthetic approaches involving MAROP. The successful deprotection of the block and random copolymers while leaving their allyl group intact has significant potential for the orthogonal functionalization of the prepared polymers. Furthermore, we demonstrated the successful use of the PEO macroinitiator, which poses its future applications in hydrogel and drug-delivery systems. Given the wide applicability of the new class of functional epoxide monomers presented in this study, we anticipate that they will contribute to the development of functionalized polyethers with potential applications in biomedical and biological fields.

ASSOCIATED CONTENT

Supporting Information

The Supporting Information is available free of charge at https://pubs.acs.org/doi/10.1021/acs.macromol.2c00761.

Additional analysis including ^{1}H, ^{13}C, COSY, and HSQC NMR, FT-IR, MALDI-ToF, GPC, and DSC data (PDF)

AUTHOR INFORMATION

Corresponding Author

Byeong-Su Kim − *Department of Chemistry, Yonsei University, Seoul 03722, Republic of Korea;* orcid.org/0000-0002-6419-3054; Email: bskim19@yonsei.ac.kr

Authors

Jihye Park − *Department of Chemistry, Yonsei University, Seoul 03722, Republic of Korea;* orcid.org/0000-0002-4592-0674

Yeji Yu − *Department of Chemistry, Yonsei University, Seoul 03722, Republic of Korea;* orcid.org/0000-0002-6880-6305

Joo Won Lee − *Department of Chemistry, Yonsei University, Seoul 03722, Republic of Korea;* orcid.org/0000-0002-3041-8411

Complete contact information is available at: https://pubs.acs.org/10.1021/acs.macromol.2c00761

Author Contributions

J.P., Y.Y., and J.W.L. contributed equally to this work.

https://doi.org/10.1021/acs.macromol.2c00761
Macromolecules 2022, 55, 5448−5458

Notes

The authors declare no competing financial interest.

■ ACKNOWLEDGMENTS

This work was supported by the National Research Foundation of Korea (NRF-2021R1A2C3004978 and NRF-2021M3H4A1A04092882).

■ REFERENCES

(1) Cho, H. Y.; Srinivasan, A.; Hong, J.; Hsu, E.; Liu, S.; Shrivats, A.; Kwak, D.; Bohaty, A. K.; Paik, H.-j.; Hollinger, J. O.; Matyjaszewski, K. Synthesis of Biocompatible PEG-Based Star Polymers with Cationic and Degradable Core for siRNA Delivery. *Biomacromolecules* **2011**, *12*, 3478−3486.

(2) Pelegri-O'Day, E. M.; Lin, E.-W.; Maynard, H. D. Therapeutic Protein−Polymer Conjugates: Advancing Beyond PEGylation. *J. Am. Chem. Soc.* **2014**, *136*, 14323−14332.

(3) Kim, M.; Mun, W.; Jung, W. H.; Lee, J.; Cho, G.; Kwon, J.; Ahn, D. J.; Mitchell, R. J.; Kim, B.-S. Antimicrobial PEGtides: A Modular Poly(ethylene glycol)-Based Peptidomimetic Approach to Combat Bacteria. *ACS Nano* **2021**, *15*, 9143−9153.

(4) Shi, S.; Yao, C.; Cen, J.; Li, L.; Liu, G.; Hu, J.; Liu, S. High-Fidelity End-Functionalization of Poly(ethylene glycol) Using Stable and Potent Carbamate Linkages. *Angew. Chem., Int. Ed.* **2020**, *59*, 18172−18178.

(5) Herzberger, J.; Niederer, K.; Pohlit, H.; Seiwert, J.; Worm, M.; Wurm, F. R.; Frey, H. Polymerization of Ethylene Oxide, Propylene Oxide, and Other Alkylene Oxides: Synthesis, Novel Polymer Architectures, and Bioconjugation. *Chem. Rev.* **2016**, *116*, 2170−2243.

(6) Mangold, C.; Wurm, F.; Frey, H. Functional PEG-based Polymers with Reactive Groups *via* Anionic ROP of Tailor-Made Epoxides. *Polym. Chem.* **2012**, *3*, 1714−1721.

(7) Isono, T.; Asai, S.; Satoh, Y.; Takaoka, T.; Tajima, K.; Kakuchi, T.; Satoh, T. Controlled/Living Ring-Opening Polymerization of Glycidylamine Derivatives Using *t*-Bu-P_4/Alcohol Initiating System Leading to Polyethers with Pendant Primary, Secondary, and Tertiary Amino Groups. *Macromolecules* **2015**, *48*, 3217−3229.

(8) Satoh, Y.; Matsuno, H.; Yamamoto, T.; Tajima, K.; Isono, T.; Satoh, T. Synthesis of Well-Defined Three- and Four-Armed Cage-Shaped Polymers via "Topological Conversion" from Trefoil- and Quatrefoil-Shaped Polymers. *Macromolecules* **2017**, *50*, 97−106.

(9) Lee, J.; Han, S.; Kim, M.; Kim, B.-S. Anionic Polymerization of Azidoalkyl Glycidyl Ethers and Post-Polymerization Modification. *Macromolecules* **2020**, *53*, 355−366.

(10) Lee, B. F.; Kade, M. J.; Chute, J. A.; Gupta, N.; Campos, L. M.; Fredrickson, G. H.; Kramer, E. J.; Lynd, N. A.; Hawker, C. J. Poly(allyl glycidyl ether)-A Versatile and Functional Polyether Platform. *J. Polym. Sci. A: Polym. Chem.* **2011**, *49*, 4498−4504.

(11) Hong, Y.; Kim, J.-M.; Jung, H.; Park, K.; Hong, J.; Choi, S.-H.; Kim, B.-S. Facile Synthesis of Poly(ethylene oxide)-Based Self-Healable Dynamic Triblock Copolymer Hydrogels. *Biomacromolecules* **2020**, *21*, 4913−4922.

(12) Illy, N.; Corcé, V.; Zimbron, J.; Molinié, V.; Labourel, M.; Tresset, G.; Degrouard, J.; Salmain, M.; Guégan, P. pH-Sensitive Poly(ethylene glycol)/Poly(ethoxyethyl glycidyl ether) Block Copolymers: Synthesis, Characterization, Encapsulation, and Delivery of a Hydrophobic Drug. *Macromol. Chem. Phys.* **2019**, *220*, 1900210.

(13) Niederer, K.; Schüll, C.; Leibig, D.; Johann, T.; Frey, H. Catechol Acetonide Glycidyl Ether (CAGE): A Functional Epoxide Monomer for Linear and Hyperbranched Multi-Catechol Functional Polyether Architectures. *Macromolecules* **2016**, *49*, 1655−1665.

(14) Song, J.; Palanikumar, L.; Choi, Y.; Kim, I.; Heo, T.-y.; Ahn, E.; Choi, S.-H.; Lee, E.; Shibasaki, Y.; Ryu, J.-H.; Kim, B.-S. The Power of the Ring: a pH-responsive Hydrophobic Epoxide Monomer for Superior Micelle Stability. *Polym. Chem.* **2017**, *8*, 7119−7132.

(15) Son, I.; Lee, Y.; Baek, J.; Park, M.; Han, D.; Min, S. K.; Lee, D.; Kim, B.-S. pH-Responsive Amphiphilic Polyether Micelles with Superior Stability for Smart Drug Delivery. *Biomacromolecules* **2021**, *22*, 2043−2056.

(16) Hans, M.; Keul, H.; Moeller, M. Chain Transfer Reactions Limit the Molecular Weight of Polyglycidol Prepared *via* Alkali Metal Based Initiating Systems. *Polymer* **2009**, *50*, 1103−1108.

(17) Stolarzewicz, A. A New Chain Transfer Reaction in the Anionic Polymerization of 2,3-Epoxypropyl Phenyl Ether and Other Oxiranes. *Macromol. Chem. Phys.* **1986**, *187*, 745−752.

(18) Brocas, A.-L.; Cendejas, G.; Caillol, S.; Deffieux, A.; Carlotti, S. Controlled Synthesis of Polyepichlorohydrin with Pendant Cyclic Carbonate Functions for Isocyanate-Free Polyurethane Networks. *J. Polym. Sci. A: Polym. Chem.* **2011**, *49*, 2677−2684.

(19) Linker, O.; Blankenburg, J.; Maciol, K.; Bros, M.; Frey, H. Ester Functional Epoxide Monomers for Random and Gradient Poly(ethylene glycol) Polyelectrolytes with Multiple Carboxylic Acid Moieties. *Macromolecules* **2020**, *53*, 3524−3534.

(20) Kwon, G.; Kim, M.; Jung, W. H.; Park, S.; Tam, T.-T. H.; Oh, S.-H.; Choi, S.-H.; Ahn, D. J.; Lee, S.-H.; Kim, B.-S. Designing Cooperative Hydrogen Bonding in Polyethers with Carboxylic Acid Pendants. *Macromolecules* **2021**, *54*, 8478−8487.

(21) Teng, K.; An, Q.; Chen, Y.; Zhang, Y.; Zhao, Y. Recent Development of Alginate-Based Materials and Their Versatile Functions in Biomedicine, Flexible Electronics, and Environmental Uses. *ACS Biomater. Sci. Eng.* **2021**, *7*, 1302−1337.

(22) Kim, H.; Shin, M.; Han, S.; Kwon, W.; Hahn, S. K. Hyaluronic Acid Derivatives for Translational Medicines. *Biomacromolecules* **2019**, *20*, 2889−2903.

(23) Liu, K.; Wei, S.; Song, L.; Liu, H.; Wang, T. Conductive Hydrogels—A Novel Material: Recent Advances and Future Perspectives. *J. Agric. Food Chem.* **2020**, *68*, 7269−7280.

(24) Paluck, S. J.; Nguyen, T. H.; Maynard, H. D. Heparin-Mimicking Polymers: Synthesis and Biological Applications. *Biomacromolecules* **2016**, *17*, 3417−3440.

(25) Liang, J.; Karakoçak, B. B.; Struckhoff, J. J.; Ravi, N. Synthesis and Characterization of Injectable Sulfonate-Containing Hydrogels. *Biomacromolecules* **2016**, *17*, 4064−4074.

(26) Smith, S. A.; Mutch, N. J.; Baskar, D.; Rohloff, P.; Docampo, R.; Morrissey, J. H. Polyphosphate Modulates Blood Coagulation and Fibrinolysis. *Proc. Natl. Acad. Sci. U. S. A.* **2006**, *103*, 903−908.

(27) Rao, N. N.; Gómez-García, M. R.; Kornberg, A. Inorganic Polyphosphate: Essential for Growth and Survival. *Annu. Rev. Biochem.* **2009**, *78*, 605−647.

(28) Lu, X.; Chen, J.; Guo, Z.; Zheng, Y.; Rea, M. C.; Su, H.; Zheng, X.; Zheng, B.; Miao, S. Using Polysaccharides for the Enhancement of Functionality of Foods: A Review. *Trends Food Sci. Technol.* **2019**, *86*, 311−327.

(29) Ko, J.; Kang, H. J.; Ahn, J.; Zhao, Z.-J.; Jeong, Y.; Hwang, S. H.; Bok, M.; Jeon, S.; Gu, J.; Ha, J.-H.; Rho, J.; Jeong, J.-H.; Park, I. Biocompatible Nanotransfer Printing Based on Water Bridge Formation in Hyaluronic Acid and Its Application to Smart Contact Lenses. *ACS Appl. Mater. Interfaces* **2021**, *13*, 35069−35078.

(30) Liu, B.; Li, F.; Niu, P.; Li, H. Tough Adhesion of Freezing- and Drying-Tolerant Transparent Nanocomposite Organohydrogels. *ACS Appl. Mater. Interfaces* **2021**, *13*, 21822−21830.

(31) Lunn, D. J.; Seo, S.; Lee, S.-H.; Zerdan, R. B.; Mattson, K. M.; Treat, N. J.; McGrath, A. J.; Gutekunst, W. R.; Lawrence, J.; Abdilla, A.; Anastasaki, A.; Knight, A. S.; Schmidt, B. V. K. J.; Bates, M. W.; Clark, P. G.; DeRocher, J. P.; Van Dyk, A. K.; Hawker, C. J. Scalable Synthesis of an Architectural Library of Well-Defined Poly(acrylic acid) Derivatives: Role of Structure on Dispersant Performance. *J. Polym. Sci. A: Polym. Chem.* **2019**, *57*, 716−725.

(32) Ranjbari, E.; Bazgir, S.; Shirazi, M. M. A. Needleless Electrospinning of Poly(acrylic acid) Superabsorbent: Fabrication, Characterization and Swelling Behavior. *Polym. Test.* **2020**, *84*, 106403.

(33) Xue, Y.-N.; Huang, Z.-Z.; Zhang, J.-T.; Liu, M.; Zhang, M.; Huang, S.-W.; Zhuo, R.-X. Synthesis and Self-Assembly of Amphiphilic Poly(acrylic acid-*b*-$_{DL}$-lactide) to Form Micelles for pH-responsive Drug Delivery. *Polymer* **2009**, *50*, 3706−3713.

https://doi.org/10.1021/acs.macromol.2c00761
Macromolecules 2022, 55, 5448−5458

(34) Qi, X.; Wei, W.; Li, J.; Liu, Y.; Hu, X.; Zhang, J.; Bi, L.; Dong, W. Fabrication and Characterization of a Novel Anticancer Drug Delivery System: Salecan/Poly(methacrylic acid) Semi-interpenetrating Polymer Network Hydrogel. *ACS Biomater. Sci. Eng.* **2015**, *1*, 1287−1299.
(35) Obermeier, B.; Frey, H. Poly(ethylene glycol-co-allyl glycidyl ether)s: A PEG-Based Modular Synthetic Platform for Multiple Bioconjugation. *Bioconjugate Chem.* **2011**, *22*, 436−444.
(36) Christ, E.-M.; Herzberger, J.; Montigny, M.; Tremel, W.; Frey, H. Poly(THF-co-cyano ethylene oxide): Cyano Ethylene Oxide (CEO) Copolymerization with THF Leading to Multifunctional and Water-Soluble PolyTHF Polyelectrolytes. *Macromolecules* **2016**, *49*, 3681−3695.
(37) Pridgen, L. N.; Miller, G. Synthesis of 2-(α-hydroxyalkyl)-1,3-Heterocyclic Alcohols and Aryl Carbamates. *J. Heterocycl. Chem.* **1983**, *20*, 1223−1230.
(38) Tauhardt, L.; Kempe, K.; Gottschaldt, M.; Schubert, U. S. Poly(2-oxazoline) Functionalized Surfaces: from Modification to Application. *Chem. Soc. Rev.* **2013**, *42*, 7998−8011.
(39) Olsén, P.; Borke, T.; Odelius, K.; Albertsson, A.-C. ε-Decalactone: A Thermoresilient and Toughening Comonomer to Poly($_L$-lactide). *Biomacromolecules* **2013**, *14*, 2883−2890.
(40) Song, J.; Hwang, E.; Lee, Y.; Palanikumar, L.; Choi, S.-H.; Ryu, J.-H.; Kim, B.-S. Tailorable Degradation of pH-responsive All Polyether Micelles *via* Copolymerisation with Varying Acetal Groups. *Polym. Chem.* **2019**, *10*, 582−592.
(41) Puchelle, V.; Du, H.; Illy, N.; Guégan, P. Polymerization of Epoxide Monomers Promoted by *t*BuP$_4$ Phosphazene Base: a Comparative Study of Kinetic Behavior. *Polym. Chem.* **2020**, *11*, 3585−3592.
(42) Sakakibara, K.; Nakano, K.; Nozaki, K. Regioregular Polymerization of Fluorine-Containing Epoxides. *Macromolecules* **2007**, *40*, 6136−6142.
(43) Kühnel, E.; Laffan, D. D. P.; Lloyd-Jones, G. C.; Martínez del Campo, T.; Shepperson, I. R.; Slaughter, J. L. Mechanism of Methyl Esterification of Carboxylic Acids by Trimethylsilyldiazomethane. *Angew. Chem., Int. Ed.* **2007**, *46*, 7075−7078.
(44) Fox, T. G. Influence of Diluent and of Copolymer Composition on the Glass Temperature of a Polymer System. *Bull. Am. Phys. Soc.* **1956**, *1*, 123.
(45) Beckingham, B. S.; Sanoja, G. E.; Lynd, N. A. Simple and Accurate Determination of Reactivity Ratios Using a Nonterminal Model of Chain Copolymerization. *Macromolecules* **2015**, *48*, 6922−6930.

https://doi.org/10.1021/acs.macromol.2c00761
Macromolecules 2022, 55, 5448−5458